ELSEVIER

International Biodeterioration & Biodegradation 49 (2002) 235–243

INTERNATIONAL BIODETERIORATION & BIODEGRADATION

www.elsevier.com/locate/ibiod

Microbially initiated pitting on 316L stainless steel

M. Geiser[a], R. Avci[b], Z. Lewandowski[c,*]

[a] Center for Biofilm Engineering, Montana State University, PO Box 3980, Bozeman, MT 59717-3980, USA
[b] Department of Physics and Image and Chemical Analysis Laboratory, Montana State University, PO Box 3980, Bozeman, MT 59717-3980, USA
[c] Department of Civil Engineering and the Center for Biofilm Engineering, Montana State University, PO Box 3980, Bozeman, MT 59717-3980, USA

Abstract

Pitting corrosion of 316L stainless steel ennobled in the presence of manganese-oxidizing bacteria, *Leptothrix discophora*, was studied in a low-concentration sodium chloride solution. Corrosion coupons were first exposed to the microorganisms in a batch reactor until ennoblement occurred, then sodium chloride was added, which initiated pitting. The pits had aspect ratios (length divided by width) and shapes closely resembling the aspect ratio and the shape of the bacteria, which suggested that the microorganisms were involved in pit initiation. © 2002 Published by Elsevier Science Ltd.

Keywords: Pit initiation; *Leptothrix discophora*; MIC; MOB; Localized corrosion; Manganese oxides

1. Introduction

It has been demonstrated that stainless steels and other passive metals and alloys when exposed to natural waters containing manganese-oxidizing bacteria can increase their open circuit potential (OCP), a phenomenon termed ennoblement (Dickinson et al., 1997; La Fond, 1999; Little et al., 1998). The effect of microbial ennoblement on passive metals is analogous to that caused by polarizing a metal anodically using a potentiostat in which the open circuit potential may reach the pitting potential. In artificial seawater (30 g NaCl/l) (Sedriks, 1996; Szklarska-Smialowska, 1986), 316L stainless steel has a pitting potential of approximately +300 mV, which means that the OCP must reach +300 mV before pitting occurs. In natural waters, 316L maintains the OCP well below its pitting potential; therefore, the stainless steel should not pit. However, manganese-oxidizing bacteria depositing manganese oxide (MnO_2) on the surface of the stainless steel (Boogerd and Vrind, 1987) cause a positive shift in the OCP. This is because when manganese oxide is in direct electrical contact with the stainless steel, the metal exhibits the following equilibrium dissolution potential of the MnO_2:

$$MnO_{2(s)} + H^+ + e^- = MnOOH_{(s)},\ E^0 = +0.81V_{SCE},$$
$$E'_{pH=7.2} = +0.383V_{SCE}. \quad (1)$$

$$MnOOH_{(s)} + 3H^+ + e^- = Mn^{2+} + 2H_2O,$$
$$E^0 = +1.26V_{SCE},\quad E'_{pH=7.2} = +0.336V_{SCE}. \quad (2)$$

The overall reaction is

$$MnO_{2(s)} + 4H^+ + 2e^- = Mn^{2+} + 2H_2O,$$
$$E^0 = +1.28V_{SCE},\quad E'_{pH=7.2} = +0.360V_{SCE}. \quad (3)$$

The standard potentials (E^0) for Eqs. (1)–(3) were calculated using the energies of formation: $\Delta G_f^0 Mn^{2+} = -54.5$ kcal/mol, $\Delta G_f^0 \gamma MnOOH = -133.3$ kcal/mol, and $\Delta G_f^0 \gamma MnO_2 = -109.1$ kcal/mol (Dickinson et al., 1996; University Chemistry Data Tables, 1995). The formal potentials (E') were calculated at a pH of 7.2 and $[Mn^{2+}] = 10^{-6}$. It has been demonstrated that surface coverage of 6% by manganese oxides (Dickinson et al., 1996) can increase the resting potential of 316L stainless steel in a fresh water environment from −200 to +362 mV_{SCE}, a 500 mV increase, at a pH of 7.2 (Dickinson et al., 1997; Linhardt, 1998).

When studying the mechanism of ennoblement of 316L stainless steels using pure cultures of manganese-oxidizing bacteria, *Leptothrix discophora*, we have noticed oddly shaped indentations in the passive layer on the metal surface. We hypothesized that the bacteria were responsible for these indentations and that these indentations were in fact sites where corrosion pits initiated. To verify this hypothesis, we set up experiments to (1) demonstrate that

* Corresponding author. Tel.: +1-406-994-0211.
E-mail address: zl@erc.montana.edu (Z. Lewandowski).

0964-8305/02/$ - see front matter © 2002 Published by Elsevier Science Ltd.
PII: S0964-8305(02)00050-1

Leptothrix discophora were responsible for the oddly shaped indentations on the surface of the ennobled stainless steel, and (2) to show that these indentations were sites where pits were initiated.

As a material to study, we used 316L stainless steel. Coupons of the metal were polished to a very smooth texture, removing as many flaws from the surface as possible. To identify sites of interest on the surface, small squares (200 μm × 200 μm) were etched using ion milling on the polished surface. Atomic force microscopy (AFM) was then used to examine the surface bound by the squares. The metal coupons were then exposed to *Leptothrix discophora* in a batch reactor. Electrical potential of the metal, reflecting progression of the ennoblement, was monitored versus a saturated calomel reference electrode (SCE). To initiate pitting, the ennobled coupons, once covered with microbial deposits, were removed from the reactor and exposed to a sterile solution of sodium chloride. The corrosion coupons were then removed to compare pit morphology with the shape of the bacteria *Leptothrix discophora* and their surfaces were examined with a scanning electron microscope (SEM) and atomic force microscope (AFM).

2. Materials and methods

2.1. Stainless steel coupons

Stainless steel coupons 1.6 cm in diameter were cut from a 1 mm thick sheet of type 316L stainless steel purchased from Reyerson in Spokane, Washington. Coupons were mounted in polycarbonate holders with silicon gel (Dickinson et al., 1997). The holders consisted of a hollow polycarbonate tube 10 cm long with an inner diameter of 9 mm and an outer diameter of 19 mm (Fig. 1).

The coupons mounted in the holder were polished to provide a surface sufficiently void of flaws for surface analysis. They were wet-sanded with tap water on Buehler–Met II metallographic grinding disks composed of silicon carbide grit of decreasing grit sizes: 120, 240, 360, 400, and 600. After the use of each grit size, the holder and coupon were rinsed with running tap water to remove any remaining grit. We then polished the coupons using Buehler aluminum oxide powder and Buehler Micropolish II powder, each suspended in water and applied with Buehler Microcloths. We initiated polishing with suspended 5 μm aluminum oxide powder. The coupons were then rinsed with tap water. Similarly, we used 0.5 and 0.05 μm polishing powders to make a mirror surface on the stainless steel, with rinses applied when polishing was complete with each powder size.

The coupons were then removed from the holders and two squares (200 μm × 200 μm), with a small number in the corner of each for identification, were etched on their smooth surfaces (Fig. 2). The etchings were made by ion milling, with a focused Ga^+ ion beam emitted from a time-of-flight secondary ion mass spectrometer (ToF-SIMS) for 7 min at

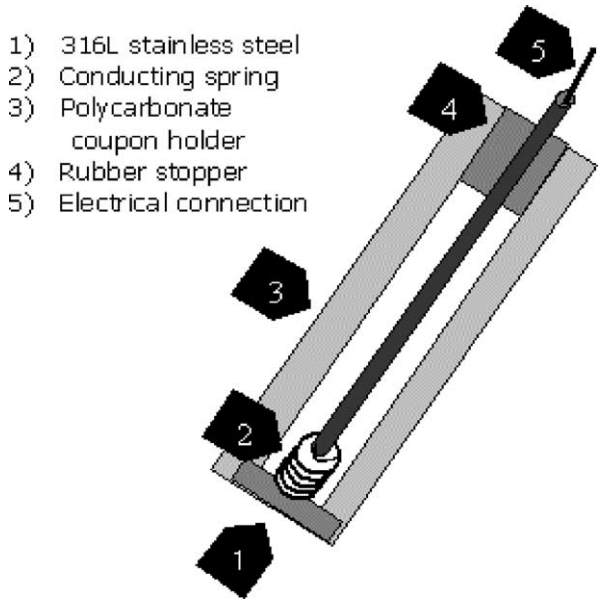

Fig. 1. Coupon holder.

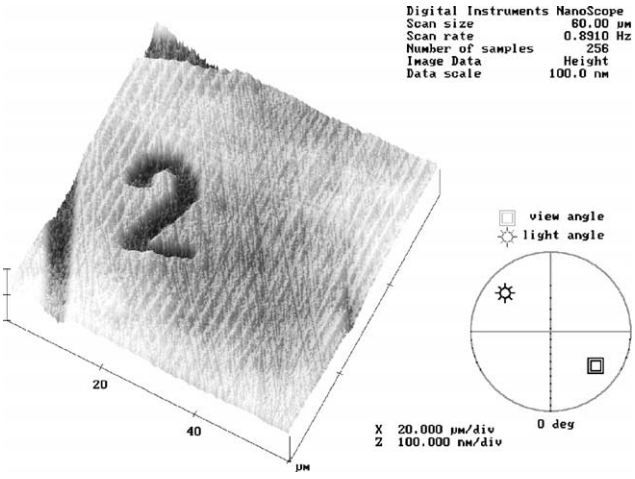

Fig. 2. Corner of the etched squares with an identification number on the surface of a polished coupon.

~ 1.5 μA ion current at 22 keV impact energy (Pendyala, 1996). The etching produced a trench in the stainless steel approximately 100 nm deep (Fig. 2). AFM was then used to map the surface of the stainless steel.

2.2. Reactor

The reactor was a polycarbonate batch cylinder reactor (Fig. 3) 10.2 cm tall and 11.1 cm in diameter. Nine polished stainless steel coupons with the etched squares were mounted to their holders again, and the holders were attached to the top of the reactor. The assembled reactor is the same as the one used by Olesen et al. (2000), though slightly modified by the addition of the reference electrode directly into the medium instead of using a salt bridge. This

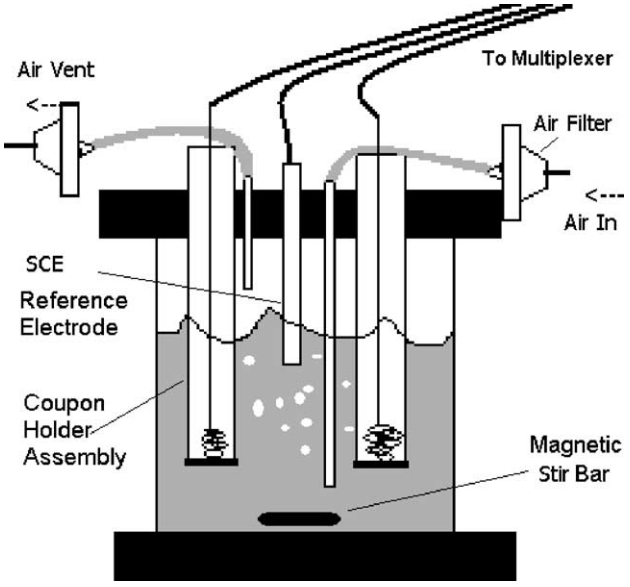

Fig. 3. Reactor.

Table 1
Composition of MSPV medium

$(NH_4)_2SO_4$	0.24 g
$MgSO_4$	0.06 g
$CaCl_2 \cdot 2H_2O$	0.06 g
KH_2PO_4	0.02 g
$Na_2HPO_4 \cdot 7H_2O$	0.05 g
HEPES	1.15 g
$FeSO_4$ 10 mM	1.0 ml
Distilled Water	1000 ml

alteration gives a much more stable potential reading. Tubes used for introducing air into the medium were mounted in the reactor, and Pall–Gelman bacterial air vents were attached to these tubes to prevent contamination of the reactor. Stirring was provided by a magnetic stir bar placed at the bottom of the reactor. The reactor was then sealed with the same silicon gel and autoclaved on dry setting (depressurization method) at 123°C and 1.2 atm for 30 min.

To prepare the growth medium, 1 litre of ATCC Culture Medium 1917 MSPV (Table 1) was autoclaved on liquid setting at 123°C and 1.2 atm for 25 min. After the medium was cooled to room temperature, we added 1 ml of syringe-filtered vitamin solution (Table 2) required by the MSPV medium, 4 ml of syringe-filtered 50 mmol manganese sulfate solution, and 5 ml of syringe-filtered 20% sodium pyruvate solution. All chemicals were from Fisher Scientific.

Manganese-oxidizing bacteria, *Leptothrix discophora* SP-6 (ATCC 51168), were obtained from ATCC and stored at −70°C. To inoculate the reactor, 150 ml of the MSPV medium containing vitamins, sodium pyruvate, and manganese sulfate was poured into a sterile 250 ml Erlenmeyer flask with the stock culture of the bacteria and placed on a

Table 2
Composition of vitamin solution

Biotin	20.0 mg
Folic Acid	20.0 mg
Thiamine Hcl	50.0 mg
D-(+)-Calcium Pantothenate	50.0 mg
Vitamin B12	1.0 mg
Riboflavin	50.0 mg
Nicotinic Acid	50.0 mg
Pyridoxine Hcl	100.0 mg
P-Aminobenzoic Acid	50.0 mg
Distilled Water	1000 ml

shaker for 2 days. Then the broth was aseptically added to the reactor along with 600 ml of the sterile medium.

Before mounting it in the reactor, the SCE reference electrode was sterilized by soaking it in 99% ethanol for 1 h. A stiff spring with a long conducting rod and stopper was connected to the coupon and coupon holder, thereby finishing the assembly (Fig. 1). The coupon assembly and reference electrode were interfaced with a computer via a Hewlett Packard 34970A Data Acquisition/Switch Unit (a multiplexer) to monitor the potential of the coupons.

The reactor was operated with the stirrer bar rotating and air bubbling through the medium until the potentials of the coupons exceeded +200 mV (see Table 3 and Fig. 4) which, according to our definition, indicated that the coupons were ennobled: This process usually took usually 5 days. Two of the nine coupons were removed from the reactor, sprayed with deionized water to remove the attached biofilm, and air-dried. These two coupons were then used to describe the surface of the coupons that were exposed to the microorganisms but not exposed to the chloride solution. The remaining coupons were also removed from the reactor, sprayed with deionized water to remove the biofilm, and then immersed in a 0.2 M NaCl solution. Spraying removed the biofilm, but it did not remove the manganese oxides on the surface. OCP of the coupons immersed in the NaCl solution was monitored, and the coupons were removed one at a time at pre-assigned intervals over the course of 2 days.

2.3. Surface analysis

Before the analysis, surfaces of all coupons were gently wiped clean with acetone and a lab tissue paper to remove the attached manganese deposits and remaining biofilm. Absence of the manganese oxides and the biofilm was verified with a light microscope, AFM, and SEM. Any remaining attached silicon gel was gently removed or coated with colloidal graphite from Ted Pella, Inc. to minimize any charging that would occur in the SEM.

SEM and AFM were used to map the surface topography of the following: (1) freshly polished sterile coupons; (2) ennobled coupons after removing microbial deposits; and (3) after exposure to the sodium chloride solution. We used a Jeol JSM-6100 scanning electron microscope with

Table 3
Highest potentials of the coupons reached. Sample 12 leaked and Sample 34 did not ennoble for an unknown reason

Sample ID	12	61	23	24	45	56	35	34	13
Potential (mV)	Leaked	224.0	301.5	282.4	299.5	251.5	267.5	165.0	217.0

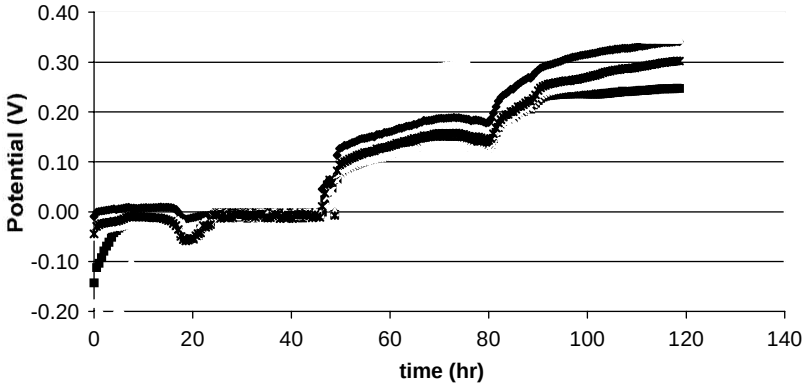

Fig. 4. Evolution of the OCP of 316L coupons exposed to manganese-oxidizing bacteria.

the beam voltage set to 15 kV. The features of interest were photographed using a Polaroid camera, type 665, at a working distance of approximately 11 mm. Using a Digital Instruments Dimension 3100 scanning probe microscope in contact mode, the surface features identified by the SEM were then mapped using an AFM.

2.4. Other tests

2.4.1. Imaging surfaces of electrochemically polarized corrosion coupons

An essential part of the project was to quantify the morphology of the pits initiated on the coupons that had been ennobled and exposed to the sodium chloride solution. The working hypothesis was that the microorganisms were involved in the pit initiation. To verify this hypothesis, we compared the morphology of pits generated in the presence of manganese-oxidizing bacteria with the morphology of pits generated by anodic polarization in sterile media. The 316L stainless steel coupons were polished as previously described and placed in an electrochemical cell with the MSPV medium, vitamins, sodium pyruvate, and manganese sulfate. Sodium chloride was then added to make a 0.1 M solution. An EG & G Princeton Applied Research Potentiostat/Galvanostat, Model 273A, was used to anodically polarize the coupons. The potential was increased at a rate of 10 V/h from -0.5 to $+0.8 V_{SCE}$ using a graphite counter electrode. Care was taken to ensure that crevice corrosion did not occur near the edge of the coupon holder (Kelly, 1995). After the applied potential exceeded the pitting potential, the coupon was removed, rinsed with deionized water, dried, and analyzed with SEM and AFM. The corrosion pits were located on the surface, and their morphology (size and aspect ratio) was quantified.

2.4.2. Imaging surfaces of sterile corrosion coupons exposed to sodium chloride

To justify our conclusions, it was necessary to show that the observed indentations in the passive layer did not form spontaneously in the sodium chloride solution. To show this, a 316L stainless steel coupon was polished, as previously described, and then cleaned with acetone and a laboratory wipe. Two squares with the same dimensions as those used in previous experiments were etched on the surface of the coupon by the same ion milling procedure. The surface of the coupon was thoroughly examined with AFM, and then the coupon was exposed to 0.2 M NaCl solution (prepared with deionized water at room temperature) and aged for $2\frac{1}{2}$ days. The coupon was then removed, rinsed with deionized water, dried, and again analyzed with AFM.

2.4.3. Imaging Leptothrix discophora attached to the surfaces of corrosion coupons

To compare the morphology of the bacteria with the morphology of the corrosion pits, we took images of the *Leptothrix discophora* attached to surfaces of corrosion coupons. Six 316L stainless steel coupons were polished to the described specification. Two 250 ml Erlenmeyer flasks each had three polished coupons placed in them. The flasks were then sealed, autoclaved for 25 min on the dry setting at 123°C and 1.2 atm, and cooled to room temperature. Two batches of MSPV medium were prepared in the same fashion as the previous experiments and autoclaved for 25 min on the dry setting at 123°C and 1.2 atm. Both batches had syringe-filtered solutions of sodium pyruvate and vitamins added, but only one had manganese sulfate added to it to make the same concentration as in the previous experiments. One sterile flask had 125 ml of the MSPV medium with manganese sulfate solution added aseptically. In the other flask, 125 ml of the MSPV media without manganese

sulfate was aseptically added. The two flasks were inoculated with *Leptothrix discophora* and shaken at room temperature. A coupon from each flask was removed and dried after 6, 8, and 10 h of bacterial growth. The coupons were gold/palladium-coated to a thickness of 15 nm and studied with the SEM.

3. Results and discussion

The potentials of the coupons in the reactor were continuously monitored against an SCE reference electrode, see Table 3 and Fig. 4.

When the ennobled coupons were placed in the sodium chloride solution, their potentials first fluctuated, indicating formation of metastable pits, then dropped, indicating that active pitting was in progress (Fig. 5).

The control run using the abiotic sodium chloride solution and sterile corrosion coupons showed that the solution of sodium chloride alone did not initiate pits on the surface of the 316L coupons as was expected (Fig. 6). Actually, the surfaces of the coupons exposed to abiotic sodium chloride became slightly smoother and had fewer scratches. The time for which the coupons were exposed to the abiotic sodium chloride exceeded the time for which the microbially colonized 316L coupons were exposed to the solution of sodium chloride. Therefore, it can be said that the sodium chloride solution alone did not initiate pitting on the surface.

AFM and SEM images (Figs. 7 and 8) illustrate pits that were formed on the surfaces of microbially colonized coupons after they were placed in sodium chloride solution. These pits formed highly organized groups of small indentations oriented in long narrow rows with smooth walls and bottom. Twenty-five of these images showed the depth of

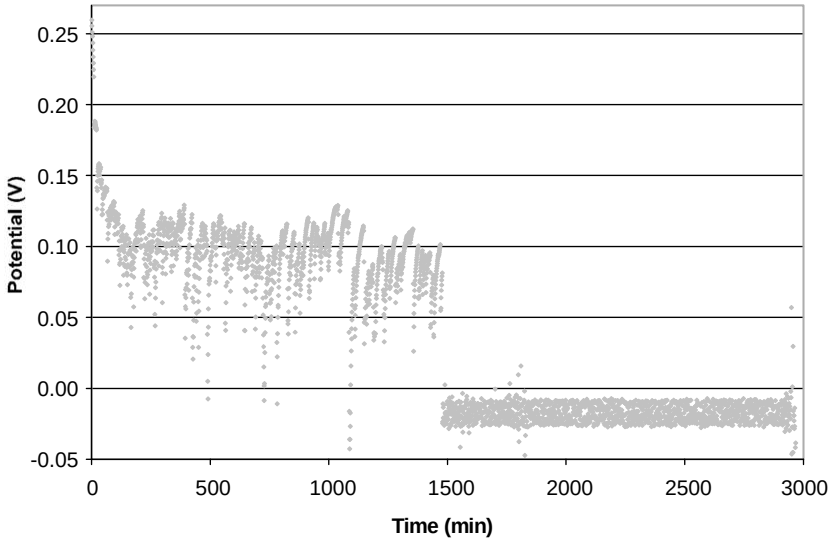

Fig. 5. Potentials measured versus SCE as a function of time.

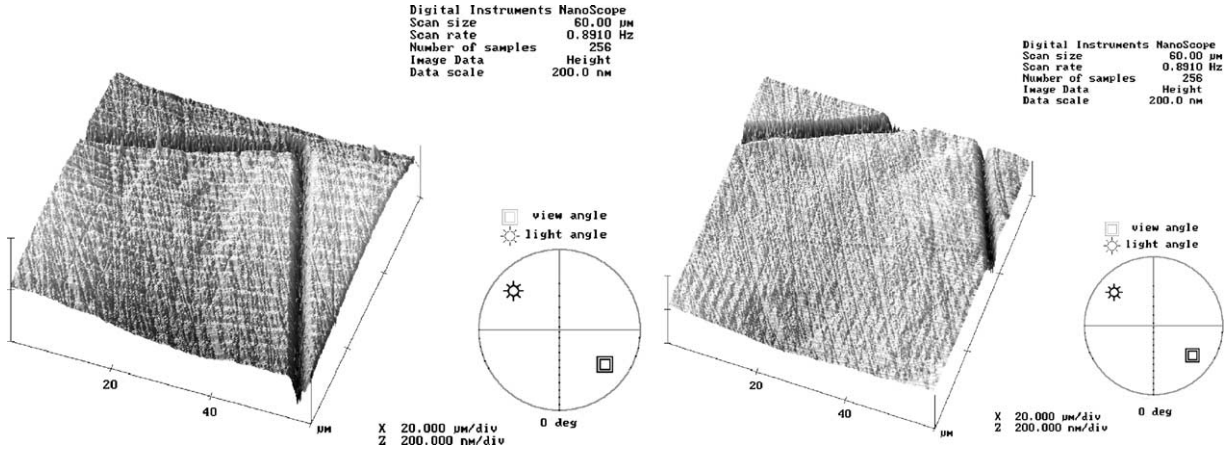

Fig. 6. AFM images of the control coupon with the etched square. Left—before experiment, Right—after experiment. Conditions: bacteria, absent; manganese, absent; chloride, 0.2 M.

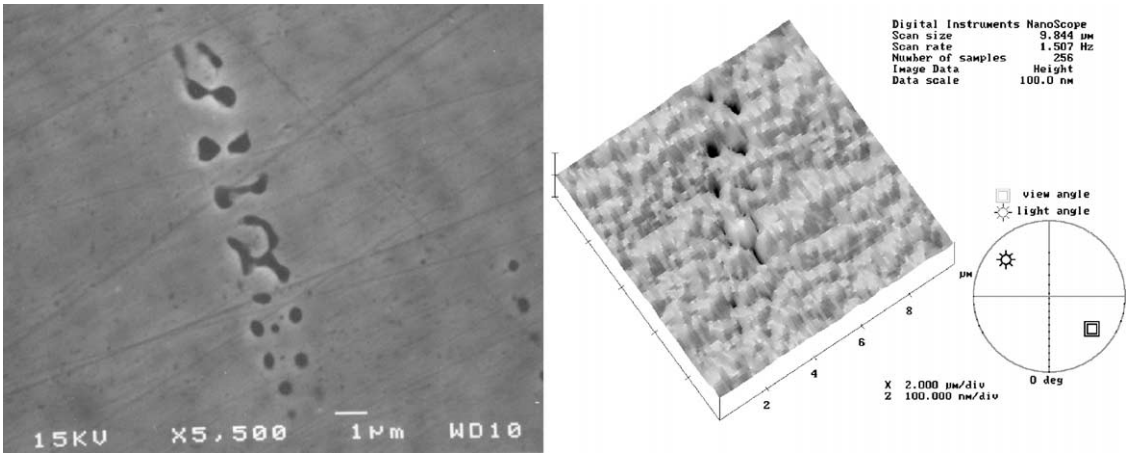

Fig. 7. Correlation between AFM and SEM of microbially initiated pits: SEM image, left; AFM image, right; Conditions: bacteria, present; manganese, present; chloride, 0.2 M.

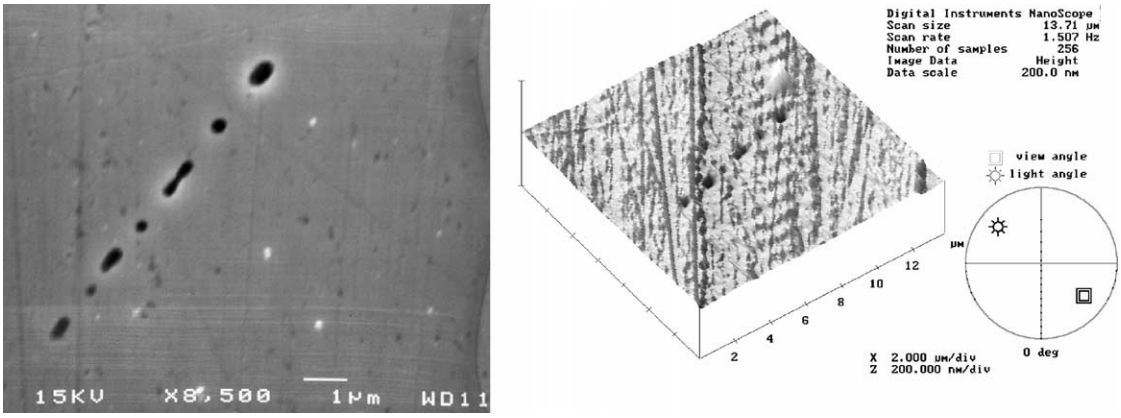

Fig. 8. A single line of organized pits in a long narrow row as seen by AFM and SEM. SEM image, left; AFM image, right. Conditions: bacteria, present; manganese, present; chloride, 0.2 M.

the pits to be 44 ± 20.51 nm, with dimensions of 12 μm long by 1.4 μm wide. Fifteen of these pits could be located with both AFM and SEM.

Fig. 9 shows SEM images of corrosion pits on anodically polarized 316L stainless steel. The pits were round and typically larger and deeper than pits initiated by bacterial colonization. Pits initiated by anodic polarization were bowl shaped with a thin metal sheath covering their mouths as previously described (Geesey et al., 1996). Our pits were on average 60.7 μm long and 50.2 μm wide. We could not use AFM to describe their shape because their depth exceeded 6.7 μm, the maximum depth the instrument could read.

Surprisingly, the two coupons removed from the reactor prior to the addition of the sodium chloride solution had similar indentations as those in Figs. 7 and 8 (Fig. 10). They were shallower, around 6 nm deep, which is approximately equal the thickness of the passive layer on stainless steels (Cunha Belo et al., 1977). Using SEM we perceived that the morphologies of pits formed in the presence of the bacteria with and without sodium chloride were similar.

To verify our hypothesis that the pits were formed at the sites occupied by the microorganisms, we took SEM images of the bacteria. To enhance visibility and prevent formation of manganese oxides, we grew the bacteria in the absence of manganese. We provide some background concerning the bacteria that were used, *Leptothrix discophora* is a cylindrical bacterium. It connects to other *Leptothrix discophora* end-to-end in a chain. Characteristically, these bacteria form a sheath of proteins and polysaccharides around them a long, narrow protective layer (Emerson and Ghiorse, 1993). The groups of bacteria in Fig. 11 are approximately 10 μm long by 1 μm wide. The agglomerates of bacteria in Fig. 11 have the same shapes as the pits on the surface of the metal (Figs. 7 and 8).

Surprisingly, even though the conditions of this test were designed to map the microorganisms, and we did not add chloride to the solution, we found indentations in the passive layer to be of similar shape to those we found in the presence of chloride (Fig. 12). These indentations had the same shape as those in Fig. 7 but were quite shallow.

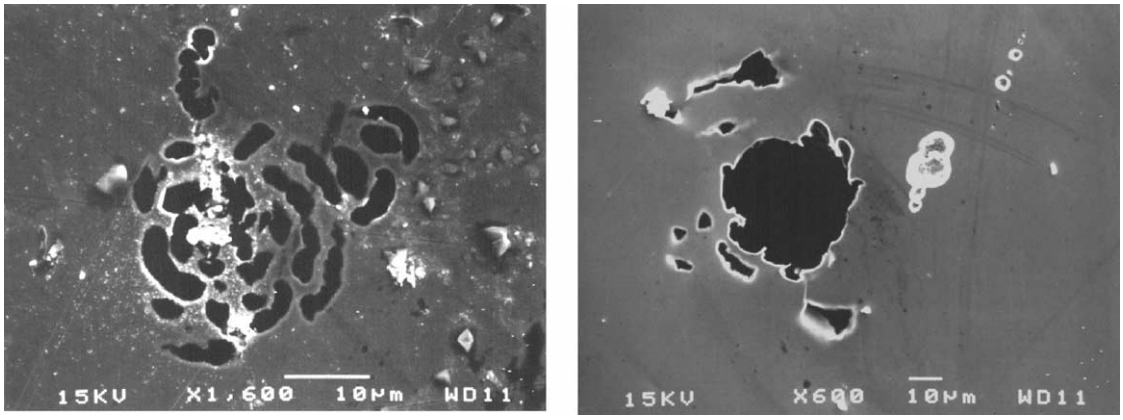

Fig. 9. SEM images of pits initiated by anodic polarization. Left, groups of holes in the thin metal sheath covering the pit's mouth; Right, small holes surrounding a large one indicating a thin metal sheath covering the pit. Conditions: bacteria, absent; manganese, present; chloride, 0.1 M.

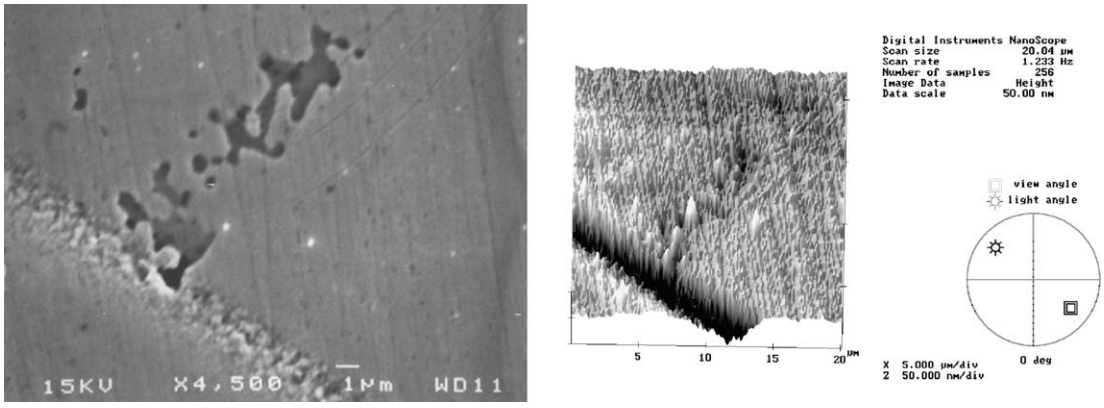

Fig. 10. Indentation on the edge of a square made by ion milling initiated by the microorganism without addition of chloride. SEM image, left; AFM image, right. Conditions: bacteria, present; manganese, present; chloride, absent.

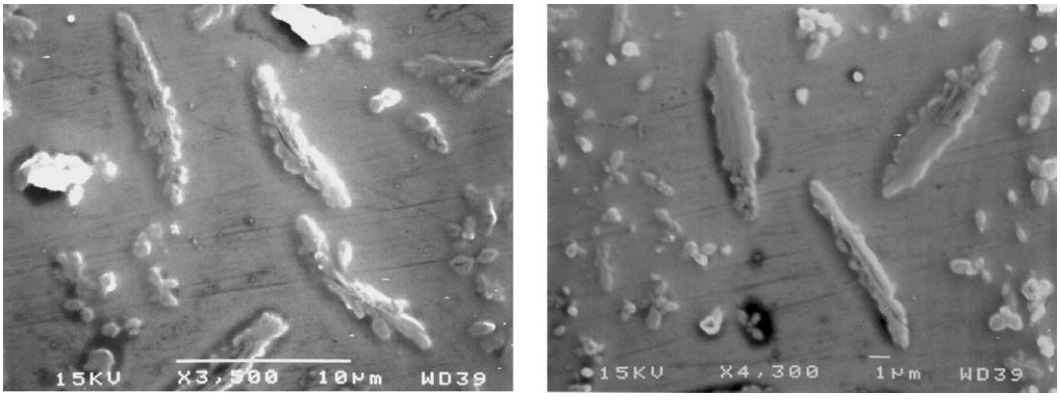

Fig. 11. SEM images of *Leptothrix discophora* grown in the absence of manganese on 316L stainless steel coupon. Conditions: bacteria, present; manganese, absent; chloride, absent.

It appears, therefore, that the pits are initiated when the bacteria are present, and the presence of chloride only accelerates their progression.

To compare the dimensions of the pits with those of the bacteria, we used an aspect ratio, the length divided by the width. To compare the sizes of the indentations in the passive layer with the sizes of microbial aggregates, we quantified the dimensions of the groups of pits (see Fig. 8 as an example). We found that the 15 pits initiated by anodic polarization had an aspect ratio of 1.28 ± 0.27, meaning they

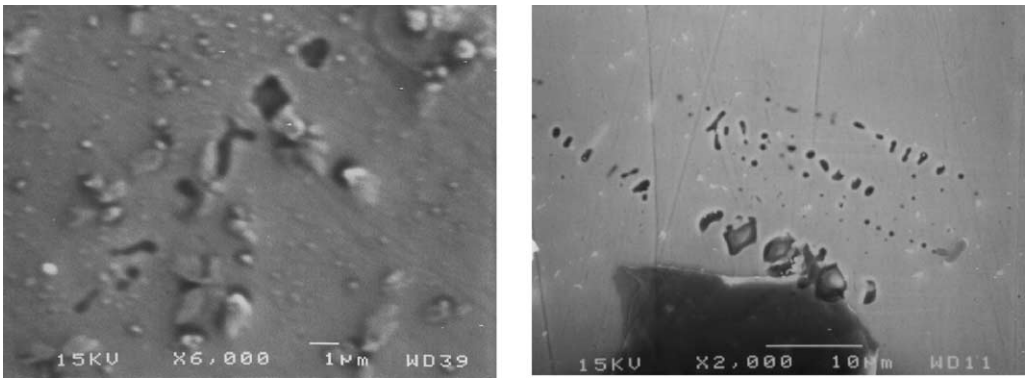

Fig. 12. Shapes with the same dimensions as those pits initiated by bacterial colonization of the surface. Left, single group of shapes; Right, groups of indentations. Conditions: bacteria, present; manganese, absent; chloride, absent.

were almost round. In contrast, 71 groups of pits found on the surface of the coupons colonized by the bacteria had an aspect ratio of 9.97 ± 5.50. Twenty groups of bacteria we measured had an aspect ratio of 10.0 ± 3.7. Both the bacteria and the pits were ten times longer than their width.

In summary, the coupons of freshly polished 316L stainless steel did not pit in an abiotic solution of sodium chloride solution. However, the same material pitted in the same chloride solution if previously microbially colonized by *Leptothrix discophora*. The formation of pits in the presence of bacteria did not require the presence of chloride. When we used the manganese-oxidizing bacteria, the pits were initiated with or without the presence of manganese. This indicates that it is the presence of the microbes, not the microbially deposited manganese oxides, that initiates pitting. The depth of the pits depends on the concentration of the chloride solution and on the time of exposure. When no chloride was present, the pits were small, and their depth was comparable with the thickness of the passive layer. When chloride was added, the pits were deeper. The pit aspect ratio (10 ± 5) and size (10 μm long by 1 μm wide) were the same for the agglomerates of bacteria and the groups of pits initiated by bacterial colonization. The standard deviations of the sizes and the aspect ratios are large for both agglomerates of the bacteria and the pits.

The manganese oxides deposited on the surface elevate the potential, creating an environment where the pits initiated by microbes cannot repassivate. In this light, it appears that the bacteria initiate the pits, and the microbially deposited manganese oxides stabilize the growth of the pits by maintaining a high potential. Further experiments will be conducted to determine the rate of the pit growth.

Finally, it is possible that pit locations are not random but pertain to features of the underlying metal substratum such as grain boundaries or crystalline phases. Geesey et al. (1996) showed a similar correlation between grain boundaries and microbial attachment that resulted in localized substratum changes. The hypothesis that the locations of microbially initiated pits are correlated with the grain boundaries will be verified in future experiments.

4. Conclusions

(1) Pits in 316L stainless steel were initiated in the presence of bacteria *Leptothrix discophora*.
(2) The presence of chloride ions made the pits deeper but was not required for the initiation of the pits. The presence of the bacteria was sufficient.
(3) We did not see any evidence of pitting when a sterile 316L stainless steel coupon was immersed in a sterile solution of sodium chloride.
(4) Pits formed in the presence of bacteria had the same sizes and aspect ratios as the agglomerates of the bacteria.
(5) Pits formed in the presence of bacteria had morphologies different from those initiated by anodic polarization of the material in the same solution.
(6) The evidences presented here indicate that the bacteria were involved in pit initiation on 316L stainless steel. However, this conclusion is based on indirect evidences—corrosion pits and microbial aggregates had the same morphology.

Further tests are needed to verify these conclusions and to determine the mechanism by which the microbes influence the integrity of passive layers.

Acknowledgements

This work was supported by United States Office of Naval Research, contract number N00014-99-1-0701 and by Cooperative Agreement EEC-8907039 between the National Science Foundation and Montana State University, Bozeman, MT, USA. We would also like to specially thank the ICAL facility of Montana State University for the use of the SEM, AFM, and ToF-SIMS.

References

Boogerd, F.C., Vrind, J.P.M.De., 1987. Manganese oxidation by *Leptothrix discophora*. Journal of Bacteriology 169, 489–494.

Cunha Belo, M., Da, Rondot, B., Pons, F., Hëricy, J.L., Langeron, J.P., 1977. Study by auger spectrometry and cathodic reduction of passive films formed on ferritic stainless steels. Journal of Elecrochemical Society September, 1317–1324.

Dickinson, W.H., Caccavo Jr., F., Lewandowski, Z., 1996. The ennoblement of stainless steel by manganic oxide biofouling. Corrosion Science 38, 1407–1421.

Dickinson, W.H., Caccavo Jr., F., Olesen, B., Lewandowski, Z., 1997. Ennoblement of stainless steel by the manganese-depositing bacterium *Leptothrix discophora*. Applied and Environmental Microbiology 63, 2502–2506.

Emerson, D., Ghiorse, W.C., 1993. Ultrastructure and chemical composition of the sheath of *Leptothrix discophora* SP-6. Journal of Bacteriology 175, 7808–7818.

Geesey, G.G., Gillis, R.J., Avci, R., Daly, D., Hamilton, M., Shope, P., Harkin, G., 1996. The influence of surface features on bacterial colonization and subsequent substratum changes of 316L stainless steel. Corrosion Science 38, 73–95.

Kelly, R.G., 1995. Pitting. Corrosion Tests and Standards: Application and Interpretation. ASTM, Philadelphia, PA, p. 168.

LaFond, R.L., 1999. Ennoblement of stainless steel in fresh water influenced by manganese oxidizing biofilms. MS Thesis, Department of Chemical Engineering, Montana State University.

Linhardt, P., 1998. Electrochemical identification of higher oxides of manganese in corrosion relevant deposits formed by microorganisms. Materials Science Forum 289–292, 1267–1274.

Little, B.J., Wagner, P.A., Lewandowski, Z., 1998. The role of biomineralization in microbiologically influenced corrosion. Corrosion, Paper 294.

Olesen, B.H., Nielsen, P.H., Lewandowski, Z., 2000. Effect of biomineralized manganese on the corrosion behavior of C1008 mild steel. Corrosion 56, 80–89.

Sedriks, AJ., 1996. Corrosion of Stainless Steels. Wiley, New York, pp. 148.

Szklarska-Smialowska, Z., 1986. Pitting Corrosion of Metals. National Association of Corrosion Engineers (NACE). p. 40–42.

Pendyala, J., 1996. Chemical effects of biofilm colonization on stainless steel. Ph.D. Thesis, Department of Physics, Montana State University.

University Chemistry Data Tables, 1995. http://www.chem.ualbetra.ca/c http://courses/plambeck/p102. p00404 and p00403.